

# Effect of a parallel magnetic field on the photocurrent in GaAs/AlAs $p-i-n$ -structures

© I.A. Larkin, Yu.N. Khanin, E.E. Vdovin<sup>✉</sup>

Institute of Microelectronics Technology and High Purity Materials, Russian Academy of Sciences,  
142432 Chernogolovka, Russia

<sup>✉</sup> E-mail: vdov62@yandex.ru

Received September 7, 2021

Revised September 16, 2021

Accepted September 16, 2021

The behavior of the photocurrent in GaAs/AlAs  $p-i-n$ -heterostructures is studied in a magnetic field parallel to the heterolayers in the wavelength range from 395 to 650 nm. A strong dependence of the non-oscillating component of the photocurrent on the radiation wavelength associated with the suppression of the diffusion current by the magnetic field was found. It is shown that the behavior of the oscillating component of the photocurrent in a magnetic field does not depend on the wavelength of light and is determined by the transfer of electrons through the dimensional quantization level in a triangular near-barrier well. It is shown that the suppression of the oscillating component by the magnetic field is due to the smearing of the level in the triangular well due to the motion of electrons parallel to the walls of the well and perpendicular to the magnetic field.

**Keywords:** heterostructures, photoconductivity, magnetotunneling.

DOI: 10.21883/SC.2022.01.53025.9738

## 1. Introduction

Under certain conditions the photoresponse of semiconductor structures can detect multiple various oscillating events. For instance, relaxation of energy of photoexcited electrons and holes due to optical phonon emission results in photocurrent oscillations depending on energy of exciting photons [1]. Multiple steps with voltage range from reverse breakdown voltage to open circuit voltage are observed at volt-ampere characteristics ( $I-V$  curves.) of InGaAs multi-step laser power converters in case of current desynchronization [2]. Photocurrent oscillations from bias voltage are also observed in  $p-i-n$ -GaAs/AlAs or InGaN/GaN superlattices [3,4]. Recently, in single-barrier GaAs/AlAs  $p-i-n$ -heterostructures the gigantic photocurrent oscillations were observed at irradiation with light with photon energy higher than forbidden band width in GaAs, which appeared as multiple resonance-like peculiarities on volt-ampere characteristics [5,6]. Absorption of light with energy higher than the forbidden band width in such semiconductor structures results in generation of electron-hole pairs. Pairs, generated in depleted  $i$ -area or at a distance of about diffusion length from  $i$ -area into the depth of doped  $n$ - and  $p$ -layers, are divided with electrical field, and as a result the current appears in external circuit [7]. Photocurrent value will be defined with drift current of carriers, generated in  $i$ -area, and diffusion currents of carriers, generated outside  $i$ -area. Such mechanism assumes the photocurrent increase with the following plateau reaching with electrical field increase in  $i$ -area and does not assume any nonmonotonic dependence. But amplitude of oscillations, experimentally observed in studies [5,6], was  $\sim 20\%$  of average value of photocurrent at irradiation with light with wavelength of  $\lambda = 650$  nm,

while in  $p-i-n$ -diodes with single tunneling barrier it is a priori impossible to assume presence of any photocurrent oscillations. These oscillations period in terms of voltage is defined with a length of  $i$ -area between AlAs-barrier and  $p^+$ -contact, and they were qualitatively interpreted in study [5] as a consequence of carriers recombination pace modulation in moments of levels coincidence of triangular quantum well  $E_n$ , forming in undoped near-barrier  $i$ -area, with bottom of conductivity band  $E_C$  of heavily doped  $p^+$ -layer with variation of electrical field, that results in sharp reduction of photocurrent. Generation of electron-hole pairs was considered in this model only in the area of electrical field existing, i.e. in  $i$ -area, while diffusion current of electrons from  $p^+$ -area and holes from  $n^+$ -area was neglected, since it was considered that time of carriers diffusion to  $i$ -area is much higher than lifetime of non-main carriers in heavily doped  $p^+$  (or  $n^+$ ) area. This assumption contradicts with the common description of photodetection in  $p-i-n$ -diodes [7], but, since it was observed, that photo-oscillations period depended on triangular quantum well width only, such model described the observed effect sufficiently realistic at lighting with wavelength of  $> 650$  nm. However, recently in study [8] the photocurrent oscillations were observed at lighting with  $\lambda = 395$  nm, that within the model, proposed in study [5], where carriers pairs generation is assumed in  $i$ -area only, the existing of the oscillating component of photocurrent is absolutely impossible, since the light absorption coefficient has spectral dependence and for purple light is about  $\alpha \sim 3 \cdot 10^5 \text{ cm}^{-1}$  [9], and majority of photons are absorbed near sample surface, not reaching the triangular quantum well.

In this study the behavior of photocurrent in magnetic field, parallel to heterolayers in GaAs/AlAs  $p-i-n$ -heterostructures in wavelength range from 395 to 650 nm

is examined. The strong dependence of non-oscillating component of photocurrent on radiation wavelength, related with diffusion current suppression with magnetic field, was observed. Behavior of oscillating component in magnetic field did not depend on light wavelength and was defined with electrons transfer through dimensional quantization level in triangular well. It is shown that suppression of the oscillating component with magnetic field is caused by level smearing in the well due to electrons moving parallel to well walls and perpendicular to magnetic field.

## 2. Samples and experimental procedure

Samples, examined by us, were made based on GaAs/AlAs  $p-i-n$ -single-barrier heterostructures with undoped  $i$ -layers with thickness of 60 and 100 nm from the side of  $p^+$ - and  $n$ -areas, respectively, grown using molecular-beam epitaxy method. Barrier level of AlAs with thickness of 5 nm is located between undoped  $i$ -layers. Upper  $p^+$ -layer of GaAs with thickness of  $0.5 \mu\text{m}$  is doped to concentration of  $2 \cdot 10^{18} \text{cm}^{-3}$ . Such structures are described in detail in studies [5,6]. Schematic band diagram of heterostructure active area at bias voltage  $V_b < 1.5 \text{V}$  ( $V_b \approx 1.5 \text{V}$  corresponds to flat bands condition) is shown in Fig. 1, *a*. Standard chemical etching technology was used for creation of optical mesastructures with diameter of  $25\text{--}200 \mu\text{m}$ . Ohmic contacts were made by means of successive evaporation of AuGe/Ni/Au layers and annealing at  $T = 400^\circ\text{C}$ . Volt-ampere characteristics were measured at noise level of  $< 100 \text{fA}$ . Measurements were made at temperature of  $4.2\text{--}100 \text{K}$ . Without lighting the reverse branches of  $I\text{--}V$  curves. presented monotonic dependencies without any visible peculiarities, dark current in interval below  $3 \text{V}$  did not exceed  $10 \text{pA}$  and was defined with the processes, similar for  $p\text{--}n$ -transition generation current. Samples were irradiated with light with wavelengths  $\lambda$  from  $650, 470$  and  $395 \text{nm}$  from the heavily doped  $p^+$ -area. Set of light-emitting diodes was used as light radiation source.

## 3. Study results and discussion

Figure 1, *b* shows  $I\text{--}V$  curves. of our experimental sample in the area of  $V_b < 1.5 \text{V}$  at lighting with  $\lambda = 650 \text{nm}$  (red points) and  $395 \text{nm}$  (purple line). Both amplitude of oscillating part of photocurrent  $I_{\text{osc}}$  and non-oscillating „background“ photocurrent  $I_{\text{non}}$  linearly depended on radiation power. It should be noted that for the non-oscillating component of photocurrent of these two lengthwaves to be almost the same, the purple light power should be increased in  $\sim 50$  times relating to red light power. Figure 1, *c* shows the curves of photons absorption for  $\lambda = 650 \text{nm}$  (red curve) and  $395 \text{nm}$  (purple curve), calculated as per formula  $\Phi \propto \Phi_0 \exp(-\alpha x)$ , where  $\Phi_0$  is the amount of photons on sample surface,  $\alpha$  is the material absorption

coefficient equal to  $\sim 3.4 \cdot 10^4 \text{cm}^{-1}$  for the red light and  $\sim 3 \cdot 10^5 \text{cm}^{-1}$  for the purple light, at  $P_{395} = 50P_{650}$  with specified vertical lines of layers boundaries of our experimental structure. To explain the scale of influence of  $\lambda$  on absorption depth it should be noted that for  $\lambda = 395 \text{nm}$  less than 1% of photons could go deep to  $p^+$ -layer to distance of  $0.2 \mu\text{m}$ , while for  $\lambda = 650 \text{nm}$  the same share of photons goes deep to  $n^+$ -layer (up to  $\sim 2 \mu\text{m}$ ), and about 15% go through both  $i$ -layers and reach boundary with  $n^+$ -layer. Thus, the observance of photocurrent oscillations at  $\lambda = 395 \text{nm}$  clearly indicates the inapplicability of their origin model presented in study [5] and necessity of its reconsideration.

Concentration of photoexcited electrons  $n_{3D}(x)$  inside the structure is described with diffusion equation

$$\frac{n_{3D}(x)}{\tau_{eA}} + D \frac{\partial^2 n_{3D}(x)}{\partial x^2} = \exp(-\alpha x) G_0, \quad (1)$$

where  $D$  is the diffusion coefficient,  $G_0$  is the electron-hole pairs generation rate,  $\tau_{eA}$  is the time of electrons recombination on holes, equal to  $\sim 1 \text{ns}$  [10]. In this model the recombination rate in  $i$ -area is negligible. Solution of equation (1), corresponding to lack of current through sample surface, is as follows

$$n_{3D}(x) = \beta G_0 \tau_{eA} \frac{\beta \exp(-\alpha x) - \alpha \exp(-\beta x)}{\beta^2 - \alpha^2}, \quad (2)$$

where  $\beta = (\tau_{eA} D)^{-1/2}$ .

This equation shows that at high radiation power the significant amount of electrons, generated in  $p^+$ -layer with thickness of  $0.5 \mu\text{m}$ , can diffuse to edge of  $p^+$ -area and then, moving ballistic in  $i$ -area, tunnel through the barrier. At the same time, in  $p^+$ -area the photoelectrons quickly thermalize by means of photons emissions and scattering on holes [11]. However, such  $n_{3D}$  electrons can not transfer to localized states  $E_j$  in triangular quantum well (TQW) due to orthogonality of wave functions of 3D electrons and wave functions of levels in a well. For such transition the scattering on phonons [12] or impurities is required. Thus, for instance, in article [13] the rate of transition from one two-dimensional layer to another two-dimensional layer by means of scattering on impurities is calculated, and it is shown that transition time is proportional to a square of energy difference of two-dimensional electrons dimensional quantization. It is reasonable to assume that the similar dependence will also be for the transition from three-dimensional states to two-dimensional by means of scattering on impurities in depleted layer. Mechanism of resonance transition to levels of virtual quantum well, limited from one side with AlAs-barrier and from another side with the sharp boundary of undoped and heavily doped area, is also possible [8,14]. Appearance of additional amount of electrons on localized or virtual levels of TQW results in photocurrent increase, i.e. each time, when with electrical field increase the new level  $E_n$  enters TQW and coincides with energy of 3D electrons, the

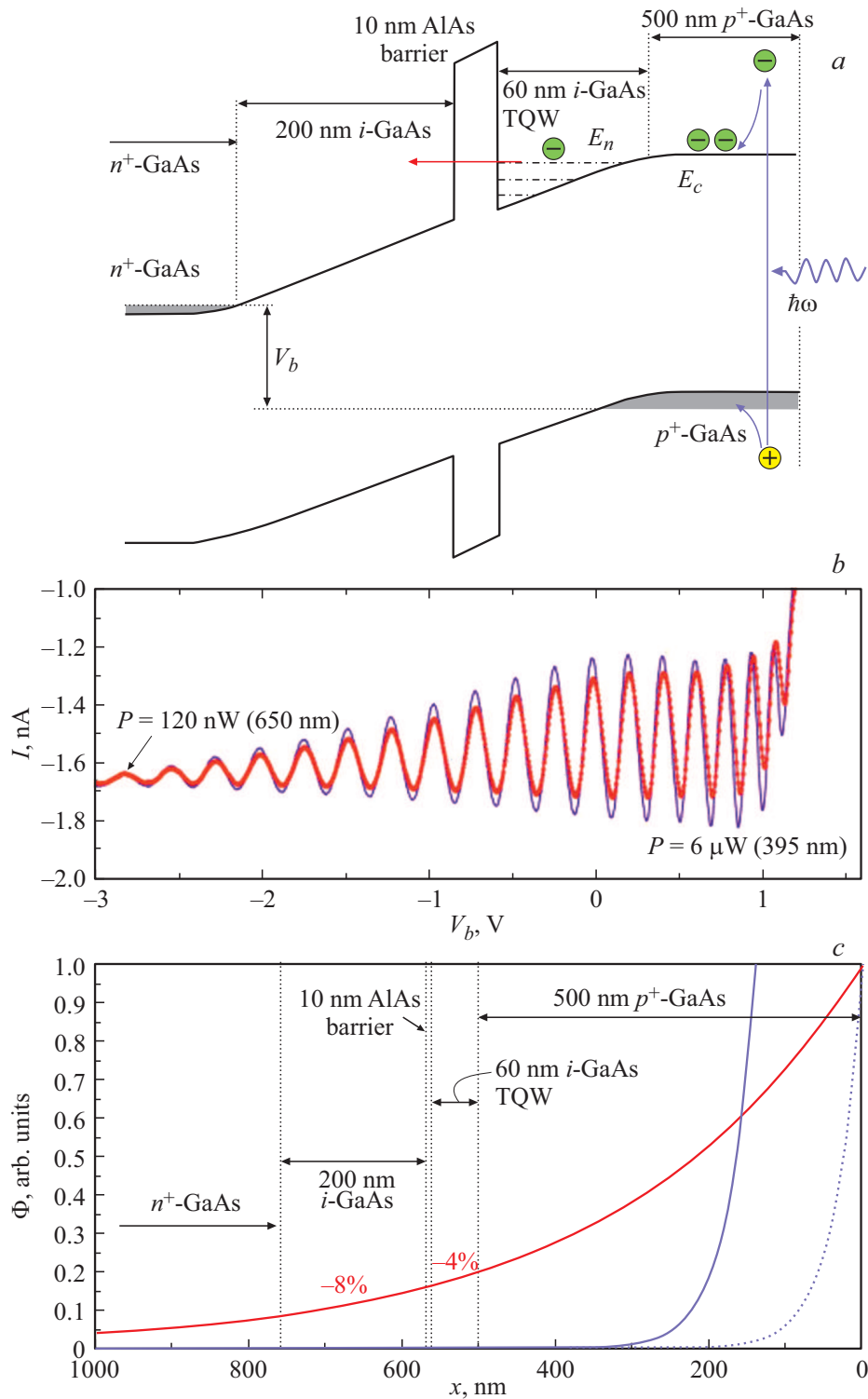


**Figure 1.** *a* — band diagram of the experimental sample at  $V_b < 1.5$  V. The arrow shows the process of electron-hole pairs photogeneration. Dashed lines are levels of dimensional quantization  $E_n$  in TQW, while  $E_c$  is the bottom of conductivity band in contact  $p^+$ -layer. Thick horizontal arrow shows resonance tunneling current through the upper level of TQW; *b* —  $I$ - $V$  curves of sample at lighting with  $\lambda = 650$  nm (red points) at  $P = 120$  nW and 395 nm (purple line) at  $P = 6$   $\mu$ W at  $T = 4.2$  K; *c* — curves of photons absorption along layers (along axis  $x$ ) of experimental structure, calculated as per formula  $\Phi \propto \Phi_0 \exp(-\alpha x)$  for  $\lambda = 650$  nm (red curve) and 395 nm (purple curves) at  $P_{395} = P_{650}$  (dashed) and at  $P_{395} = 50P_{650}$  (solid). (Colored version of the figure is presented in electronic version of the article).

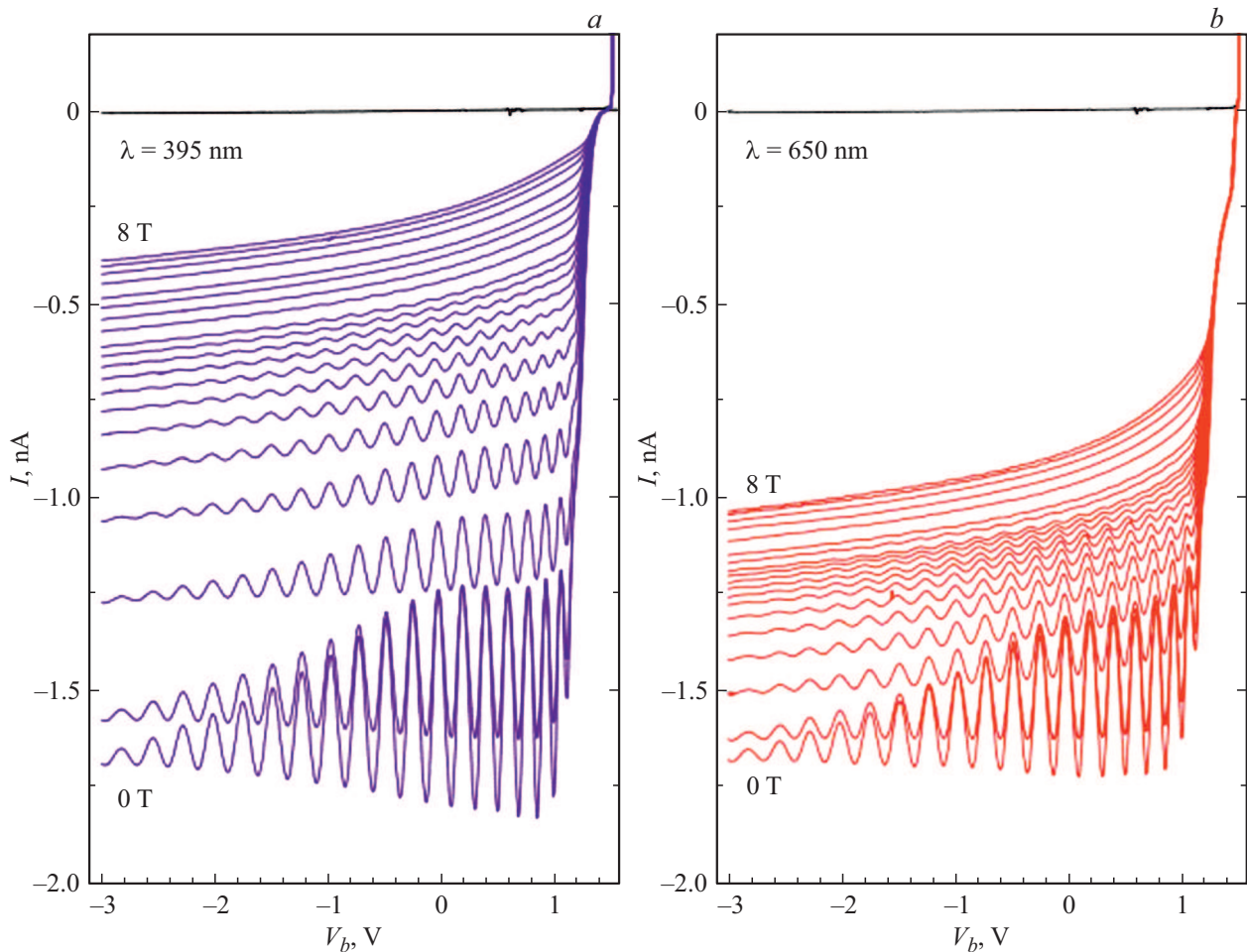


**Figure 2.**  $I$ – $V$  curves. in magnetic field, perpendicular to current  $B_z$  from 0 to 8 T for  $\lambda = 395$  nm (a) and 650 nm (b). Magnetic field step in interval from 0 to 2.2 T is 0.2 T, then one curve at 2.6 T and from 3 to 8 T, the step is 1 T. (Colored version of the figure is presented in electronic version of the article).

sharp increase of tunneling current through the barrier happens. At the same time, the oscillations amplitude is proportional to amount of electrons, transitioned to the edge of triangular quantum well from  $p^+$ -area with energy, close to  $E_c$ . Value of non-oscillating component of photocurrent includes additive contributions of current-tunneling 3D electrons and electrons and holes, excited with light of certain wavelength in all other areas of heterostructure.

Measurements of photo-oscillations behavior in magnetic field  $B_z$ , perpendicular to current, allowed to observe the independent confirmation of the presented explanation of the abovementioned model applicability. Figure 2 shows the  $I$ – $V$  curves. sets for  $\lambda = 395$  and 650 nm at the same radiation power, as in Fig. 1, b with variation of  $B_z$  in interval from 0 to 8 T, which show sharp difference of suppression of non-oscillating component of photocurrent  $I_{\text{non}}$  with magnetic field for various  $\lambda$ . Relation of effects of suppression of  $I_{\text{non}}$  and  $I_{\text{osc}}$  with increase of  $B_{\text{ort}}$  for  $\lambda = 395, 470$  and 650 nm is presented in Fig. 3. We assume that difference of suppression of  $I_{\text{non}}$  for  $\lambda = 395$  and 650 nm in Figs. 2

and 3, a can be explained within our model with essentially different spatial location in structure of processes of generation, recombination and diffusion, defining the value of  $I_{\text{non}}$ . Equation (2) shows that for  $\lambda = 650$  nm, where, as per our estimates,  $\alpha \approx \beta$ , diffusion and photogeneration contributions to concentration of electrons  $n_{3D}(x)$  are almost equal, while for  $\lambda = 395$  nm the diffusion contribution dominates. Magnetic field suppresses diffusion in  $p^+$ -area as per the law  $D(B) = D_0 / (1 + (\omega_c \tau)^2)$ , where  $\omega_c$  is the cyclotron frequency,  $\tau$  is the mean free time, but does not influence on photogeneration. According to equation (2), at diffusion, fully suppressed with magnetic field, current  $I_{\text{non}}$  for  $\lambda = 650$  nm should be in  $\sim 2$  times less, than without magnetic field, and for  $\lambda = 395$  nm  $I_{\text{non}}$  — exponentially low. Also, it should be noted that significant contribution to  $I_{\text{non}}$  for  $\lambda = 650$  nm is made by electrons and holes generated in  $i$ -area of structure and moving in strong electrical field, where influence of  $B_z$  on their ballistic transport is low and does not result in significant reduction of  $I_{\text{non}}$ . Figure 3, a shows that  $I_{\text{non}}$  with magnetic field increase to 8 T for  $\lambda = 650$  nm  $I_{\text{non}}$  decreases in  $\sim 1.5$  times, and

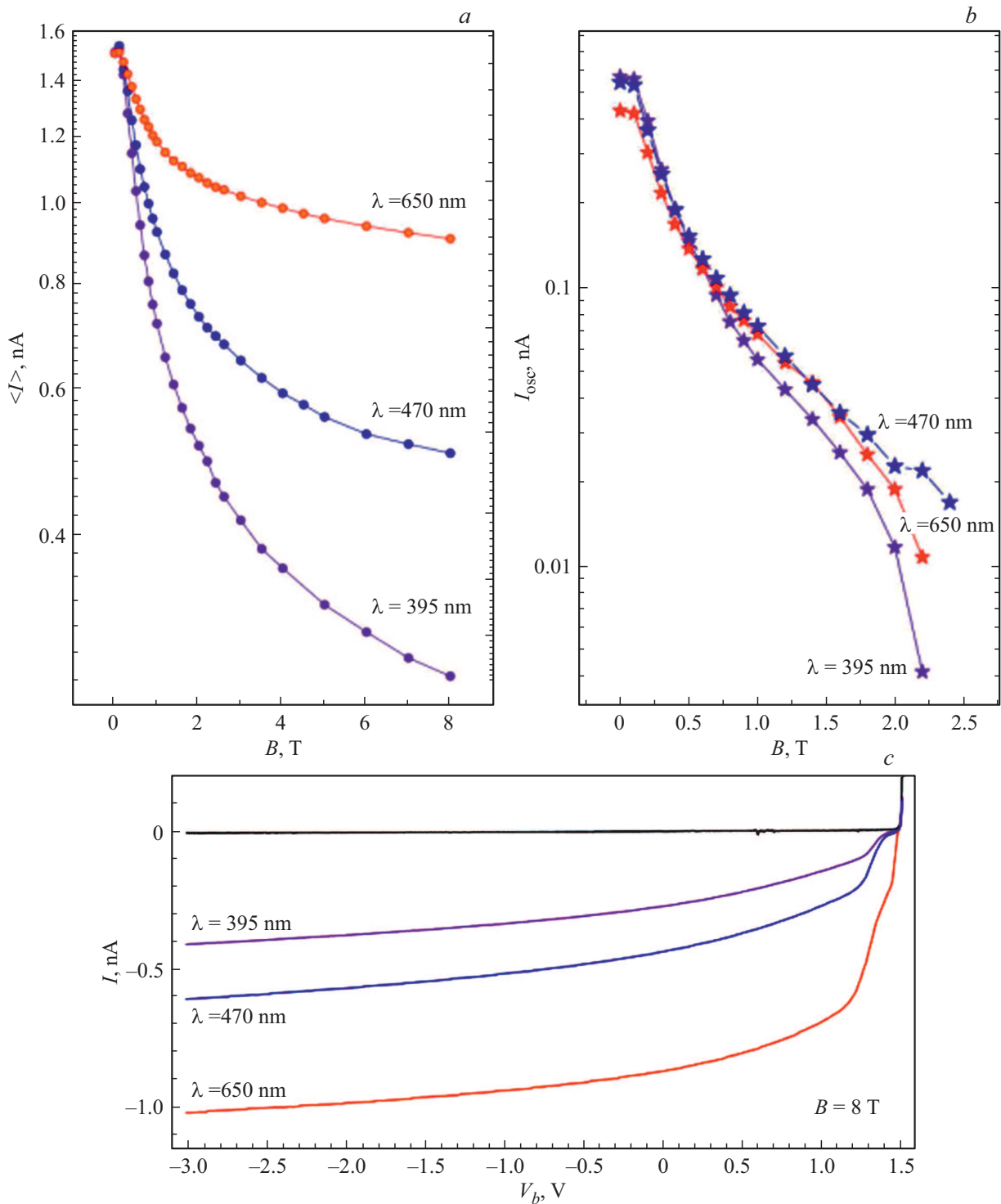


**Figure 3.** *a* — dependencies of  $I_{non}$  at  $V_b = 0$  on  $B_z$  for  $\lambda = 395$  nm (purple),  $\lambda = 470$  nm (blue) and  $\lambda = 650$  nm (red); *b* — dependencies of  $I_{osc}$  at  $V_b = 0$  on  $B_{ort}$  for  $\lambda = 395$  nm (purple),  $\lambda = 470$  nm (blue) and  $\lambda = 650$  nm (red); *c* — dependencies of  $I_{non}$  on  $V_b$  at  $B_z = 8$  T for  $\lambda = 395$  nm (purple),  $\lambda = 470$  nm (blue) and  $\lambda = 650$  nm (red). (Colored version of the figure is presented in electronic version of the article).

for  $\lambda = 395$  nm — in  $\sim 5$  times. Since for light with  $\lambda = 470$  nm (blue)  $\alpha \approx 1.1 \cdot 10^5 \text{ cm}^{-1}$  (i.e. significantly higher than for red light, but less than for purple), the dependence of  $I_{non}$  on  $B_z$  for it will be between the depen-

dependencies for red and purple light, that is observed in Fig. 3, *a*. Figure 3, *c* shows the dependencies of  $I_{non}$  on  $V_b$  at 8 T for 395, 470 and 650 nm, according to which the difference between them in interval from  $-3$  to 1 V is almost constant.

Application of field  $B_z$  (see Fig. 3, *b*) resulted in smooth and almost independent from  $\lambda$  suppression of value of  $I_{osc}$ , since the properties of electrons, localized on TQW levels, and three-dimensional electrons near boundary of  $p^+$ - and  $i$ -areas do not depend on  $\lambda$ . It should be noted that such suppression of tunneling current oscillations with magnetic field, perpendicular to layers, was observed at tunneling through two-barrier  $n-i-n$ -structures with wide quantum wells in study [15], that is also caused by Lorentz force influence on the tunneling electron. As we demonstrated above, the local maximum of photocurrent appears at approaching of the level in TQW to bottom of conductivity band in  $p^+$ -layer. Electrons movement parallel to barrier and perpendicular to magnetic field along axis  $y$  results in shift of the level in TQW  $\delta E$ :

$$\delta E = t^{-1} \int_0^d e v_y B_z x v_x^{-1} dx \approx \frac{\hbar}{3l_b^2} v_y d, \quad (3)$$

where  $l_b$  is the magnetic length,  $d$  is the TQW width,  $v_y$  and  $v_x$  are the components of electron velocity, parallel and perpendicular to layers, respectively,  $t$  is the time of ballistic transit of electrons in TQW,  $t \approx (2m^*d/F)^{1/2}$  ( $F$  is the triangular well slope). It is obvious that oscillations are suppressed, when TQW level smearing due to presence of magnetic field  $B_z$  and velocity  $v_y$ , aligns with distances between levels  $\Delta E$ , i.e.  $\delta E = \Delta E/2$ . Distance between levels in TQW in quasi-classical approximation  $\Delta E = \pi\hbar/t$ . As per our estimates, at  $\delta E = \Delta E/2$  and Gaussian distribution of velocities  $v_y$  and  $v_z$  in TQW the relative oscillations amplitude will be  $\sim 15\%$  of initial and correspond to suppression observed in the experiment (see Fig. 3, *b*) in magnetic field of  $\sim 1$  T. This result allows to evaluate the mean kinetic of electrons  $E_{yz}$  at the level in TQW, in assumption, that distribution of electrons on level is isotropic and rate of transition from 3D to TQW does not depend on magnetic field. Then

$$E_{yz} = \frac{m^*(v_y^2 + v_z^2)}{2} = \frac{9\pi^2 l_b^4 F}{2d^3}, \quad (4)$$

that is  $\sim 20$  meV. This value is significantly higher than temperature of electrons and holes in  $p^+$ -area, but almost equal to value of fluctuations of conductivity band bottom [16].

## 4. Conclusion

Thus, both photo-oscillations behavior in magnetic field and dependence of suppression of non-oscillating component of photocurrent with magnetic field for various wavelengths confirmed the applicability of our model of photo-oscillations in single-barrier GaAs/AlAs  $p-i-n$ -structures. These results can help to better understand the mechanisms of photocurrent formation in  $p-i-n$ -heterostructures and contribute to development of new solar cells, photoelectric receivers and other photoelectrical devices.

## Acknowledgments

The authors would like to thank M. Henini, University of Nottingham, UK, for samples manufacturing. The work has been performed under the state assignment No. 075-00355-21-00.

## Conflict of interest

The authors declare that they have no conflict of interest.

## References

- [1] R.E. Nahory. *Phys. Rev.*, **178**, 1293 (1969).
- [2] A.C. Wang, Y.R. Sun, S.Z. Yu, J.J. Yin, W. Zhang, J. Wang, Q.X. Fu, J.R. Dong. *Appl. Phys. Lett.*, **118**, 233902 (2021).
- [3] J. Allam, F. Capasso, M.B. Panish, A.L. Hutchinson. *Appl. Phys. Lett.*, **49**, 707 (1986).
- [4] M.V. Baranovskiy, G.F. Glinskii. *J. Phys.: Conf. Ser.*, **461**, 012039 (2013).
- [5] E.E. Vdovin, M. Ashdown, A. Patane, L. Eaves, R.P. Campion, Yu.N. Khanin, M. Henini, O. Makarovskiy. *Phys. Rev. B*, **89**, 205305 (2014).
- [6] Yu.N. Hanin, E.E. Vdovin, O. Makarovskii, M. Henini. *Pis'ma ZhETF*, **102** (11), 830, (2015) (in Russian).
- [7] S.M. Sze. *Physics of Semiconductor Devices* (N. Y., Wiley, 1981) p. 749.
- [8] E.E. Vdovin, Yu.N. Hanin. *Pis'ma ZhETF*, **113** (9), 605 (2021) (in Russian).
- [9] M.D. Sturge. *Phys. Rev.*, **129**, 2835 (1963).
- [10] W.P. Dumke. *Phys. Rev.*, **132**, 1998 (1963).
- [11] M.I. D'yakonov, V.I. Perel', I.N. Yasievich. *FTP*, **11** (7), 1364 (1977) (in Russian).
- [12] P.J. Turley, S.W. Teitsworth. *Phys. Rev. B*, **50**, 8423 (1994).
- [13] I.A. Larkin. *FTP*, **23** (9), 1664 (1989) (in Russian).
- [14] E.E. Vdovin, Yu.V. Dubrovskii, I.A. Larkin, Yu.N. Hanin, T. Andersson. *Pis'ma ZhETF*, **61** (7), 566 (1995) (in Russian).
- [15] M.L. Leadbeater, E.S. Alves, L. Eaves, M. Henini, O.H. Hughes, A. Celeste, J.C. Portal, G. Hill, M.A. Pate. *J. Phys.: Condens. Matter*, **1**, 4865 (1989).
- [16] A.L. Efros. *ZhETF*, **59**, 880 (1971) (in Russian).